Photochemical Electron Transfer in Chlorophyll–Porphyrin–Quinone Triads: The Role of the Porphyrin-Bridging Molecule

Douglas G. Johnson, Mark P. Niemczyk, David W. Minsek, Gary P. Wiederrecht, Walter A. Svec, George L. Gaines, III, and Michael R. Wasielewski*

Contribution from the Chemistry Division, Argonne National Laboratory, Argonne, Illinois 60439

Received December 17, 1992

Abstract: The photochemistry of four chlorophyll–porphyrin–naphthoquinone molecules possessing both fixed distances and orientations between the three components is described. These molecules consist of a methyl pyropheophorbide *a* or pyrochlorophyllide *a* that is directly bonded at its 3-position to the 5-position of a 2,8,12,18-tetraethyl-3,7,13,-17-tetramethylporphyrin, which is in turn bonded at its 15-position to a 2-triptycenenaphthoquinone. In addition, porphyrin–quinone compounds in which the chlorins are replaced by a *p*-tolyl group were also prepared as reference compounds. Selective metalation of the macrocycles with zinc gives the series ZCHPNQ, ZCZPNQ, HCZPNQ, HCHPNQ, HPNQ, and ZPNQ, where H, Z, C, P, and NQ denote free base, Zn derivative, chlorophyll, porphyrin, and naphthoquinone, respectively. Selective excitation of ZC in ZCZPNQ and ZCHPNQ, and HC in HCHPNQ dissolved in butyronitrile yields ZC^+ZPNQ^-, ZC^+HPNQ^-, and HC^+HPNQ^- with rate constants of 1.0×10^{11}, 9.0×10^9, and 8.2×10^9 s^{-1}, respectively, while the corresponding ion-pair recombination rate constants are 1.4×10^{10}, 4.0×10^9, and 4.0×10^9 s^{-1}, respectively. The fact that ZCZPNQ possesses faster rates of charge separation than do ZCHPNQ and HCHPNQ is inconsistent with an electron transfer mechanism involving superexchange with virtual states possessing anionic character on the bridging porphyrin. The data support an electron transfer mechanism in which the lowest excited singlet state of the bridging porphyrin weakly mixes with the lowest excited singlet state of the chlorophyll. This mixed state crosses over to a charge transfer state in which the bridging porphyrin is oxidized and the quinone is reduced. This charge transfer state then relaxes to yield the final state which possesses an oxidized chlorophyll and a reduced quinone.

Introduction

The nature of the medium that lies between the electron donors and acceptors in photosynthetic reaction centers is thought to have a large influence on the observed rates of electron transfer within these proteins.[1-3] For example, in the bacterial photosynthetic reaction center a bacteriochlorophyll (BChl) molecule lies between the dimeric bacteriochlorophyll donor ($BChl_2$) and the bacteriopheophytin (BPh) acceptor.[4-6] The π systems of these chromophores lie at large angles relative to one another (about 70°) in an approximate edge-to-edge configuration. Femtosecond transient absorption spectroscopy of native reaction centers has yielded evidence for two basic mechanisms of electron transfer involving this accessory BChl. Initial measurements indicated that an electron is transferred in a single 3-ps step from $^1*BChl_2$ to BPh.[7-9] However, within the context of semiclassical electron transfer theory, the large rate constant for this reaction is incompatible with the 17-Å distance over which the electron transfer occurs. Nevertheless, mixing low-lying ionic states of the intermediate BChl with those of the $^1*BChl_2$ donor and BPh acceptor may lead to a greatly increased rate of charge separation.[1-3] This concept, known as superexchange, has its origins in the work of Kramers.[10] McConnell has used this concept to describe electron transfer between aromatic molecules across a hydrocarbon spacer.[11] This idea has been elaborated further by other workers who have investigated the dependence of electron transfer rates on the energies and spatial characteristics of both hydrocarbon[12-15] and protein spacer orbitals.[16-20] These concepts and how they relate to photosynthetic charge separation have been discussed in a recent review.[2]

More recently, Zinth et al.[21,22] have found complex kinetics in the Q_y region of the transient absorption spectra of bacterial reaction centers that they interpret as evidence for the appearance of $BChl^-$ as a distinct chemical intermediate, which forms with $\tau = 3.5$ ps and disappears with $\tau = 0.9$ ps. Kirmaier and Holten[23] have criticized Zinth's interpretation based on their ideas that variations in the reaction center transient absorption kinetics may be due to an inhomogeneous ensemble of reaction center proteins. A third view suggests that both one- and two-step mechanisms may be involved in the electron transfer process depending on the energy level of the $BChl_2^+$ $BChl^-$ state relative to that of $^1*BChl_2$. The relative contribution of each mechanism to the overall electron transfer process is temperature dependent.[24,25]

In general, molecules possessing low-lying π molecular orbitals that can mix significantly with the HOMO of the donor and the

(1) Marcus, R. A. *Chem. Phys. Lett.* **1988**, *133*, 471.
(2) Won, Y.; Friesner, R. A. *Biochim. Biophys. Acta* **1988**, *935*, 9.
(3) Bixon, M.; Jortner, J.; Plato, M.; Michel-Beyerle, M. E. In *The Bacterial Reaction Center, Structure and Dynamics*; Breton, J., Vermeglio, A., Eds.; Plenum: New York, 1988; pp 399–419.
(4) Deisenhofer, J.; Epp, O.; Miki, K.; Huber, R.; Michel, H. *J. Mol. Biol.* **1984**, *180*, 385.
(5) Chang, C.-H.; Tiede, D.; Tang, J.; Smith, U.; Norris, J.; Schiffer, M. *FEBS Lett.* **1986**, *205*, 82.
(6) Allen, J. P.; Feher, G.; Yeates, T.-O.; Komiya, H.; Rees, D. C. *Proc. Natl. Acad. Sci. U.S.A.* **1987**, *84*, 6162.
(7) Wasielewski, M. R.; Tiede, D. *FEBS Lett.* **1986**, *204*, 368.
(8) Martin, J.-L.; Breton, J.; Hoff, A.; Migus, A.; Antonetti, A. *Proc. Natl. Acad. Sci. U.S.A.* **1986**, *83*, 957.
(9) Breton, J.; Martin, J. L.; Migus, A.; Antonetti, A.; Orszag, A. *Proc. Natl. Acad. Sci. U.S.A.* **1986**, *83*, 5121.
(10) Kramers, H. D. *Physica* **1934**, *1*, 152.
(11) McConnell, H. M. *J. Chem. Phys.* **1961**, *35*, 508.
(12) Paddon-Row, M. N. *Acc. Chem. Res.* **1982**, *15*, 245.
(13) Ohta, K.; Closs, G. L.; Morokuma, K.; Green, N. J. *J. Am. Chem. Soc.* **1986**, *108*, 1319.
(14) Beratan, D. N.; Hopfield, J. J. *J. Am. Chem. Soc.* **1984**, *106*, 1584.
(15) Larsson, S.; Volosov, A. *J. Chem. Phys.* **1986**, *85*, 2548.
(16) Larsson, S. *J. Am. Chem. Soc.* **1981**, *103*, 4034.
(17) Larsson, S. *J. Chem. Soc., Faraday Trans. 2* **1983**, *79*, 1375.
(18) Redi, M.; Hopfield, J. J. *J. Chem. Phys.* **1980**, *72*, 6651.
(19) Marcus, R. A. *Chem. Phys. Lett.* **1988**, *146*, 13.
(20) Joachim, C. *Chem. Phys.* **1987**, *116*, 339.
(21) Holzapfel, W.; Finkele, U.; Kaiser, W.; Oesterhelt, D.; Scheer, H.; Stilz, H. U.; Zinth, W. *Chem. Phys. Lett.* **1989**, *160*, 1.
(22) Dressler, K.; Umlauf, E.; Schmidt, S.; Hamm, P.; Zinth, W.; Buchanan, S.; Michel, H. *Chem. Phys. Lett.* **1991**, *183*, 270.
(23) Kirmaier, C.; Holten, D. *Biochemistry* **1991**, *30*, 609.

0002-7863/93/1515-5692$04.00/0

LUMO of the acceptor may enhance the rate of electron transfer from the donor to the acceptor via superexchange. For example, aromatic amino acids, such as tyrosine, phenylalanine, and tryptophan, positioned between an electron donor and an acceptor in proteins, may facilitate electron transfer reactions. Unfortunately, there are few experimental tests of superexchange in structurally well-defined donor–acceptor molecules, especially those involving excited state electron transfers.[26-30] The problem lies in producing a series of rigid donor–acceptor molecules in which the effects of changing the orbital energies of the intervening spacer molecule are not convolved with changes in conformation.

Sessler et al.[28,29] have recently reported an interesting series of rigid porphyrin–porphyrin–quinone triads that implicate states involving the central porphyrin in electron transfer between the terminal porphyrin and the quinone. The two porphyrins that comprise these triads are electronically very similar. One way to distinguish between them to some degree is to selectively metalate one of the macrocycles. Rodriguez et al.[29] report on the photophysics of the triads in which the porphyrin that is either proximal or distal to the quinone is metalated. When the proximally metalated derivative is excited at 582 nm with 350 fs laser flashes, two processes are observed. First, a fast charge separation–recombination occurs between the zinc porphyrin and the quinone. Second, a slower 55–75-ps process attributable to deactivation of the free-base excited state to ground state by the presence of the quinone occurs. The time constant for this process is weakly temperature dependent and independent of solvent. This result is interpreted as superexchange mediated electron transfer from free-base to quinone. Excitation of the distally metalated isomers results in behavior that is attributed to electron transfer from free-base to the quinone followed by charge recombination that occurs in less than 15 ps.

Osuka et al.[30-32] have developed models of photosynthetic reaction center pigments consisting of 2, 3, and 4 porphyrins with an individual benzoquinone or pyromellitimide acceptor attached to the terminal porphyrin. Two porphyrins are stacked to act like the special pair dimer in photosynthetic systems. Fluorescence quenching in each molecule relative to the monomer porphyrin was >90%, suggesting an additional non-radiative path to ground state. The authors showed that rapid electron transfer occurs between the porphyrin and the acceptor that are adjacent to one another. This electron transfer may be followed by a second dark electron transfer from the dimeric porphyrin to the central oxidized porphyrin. In these molecules it is difficult to selectively excite the terminal porphyrin dimer to test whether the bridging porphyrin can function as a virtual intermediate in a superexchange mechanism for electron transfer from the dimer to the acceptor.

To study superexchange involving aromatic molecules we recently prepared a series of rigid, fixed-distance porphyrin–spacer–quinone molecules[33] in which the spacer is pentiptycene,[34] a hydrocarbon which consists of two triptycene molecules that share a common central benzene ring. The π systems of the donor, the central benzene ring of the pentiptycene spacer, and the acceptor are isolated from one another by saturated hydrocarbon bridges. The central benzene ring of the spacer allows one to use substituents on the remaining two free positions of this ring to alter the energy of the HOMO and LUMO of the aromatic spacer. This alters the relative contribution of ionic states of the spacer to a superexchange description of electron transfer.

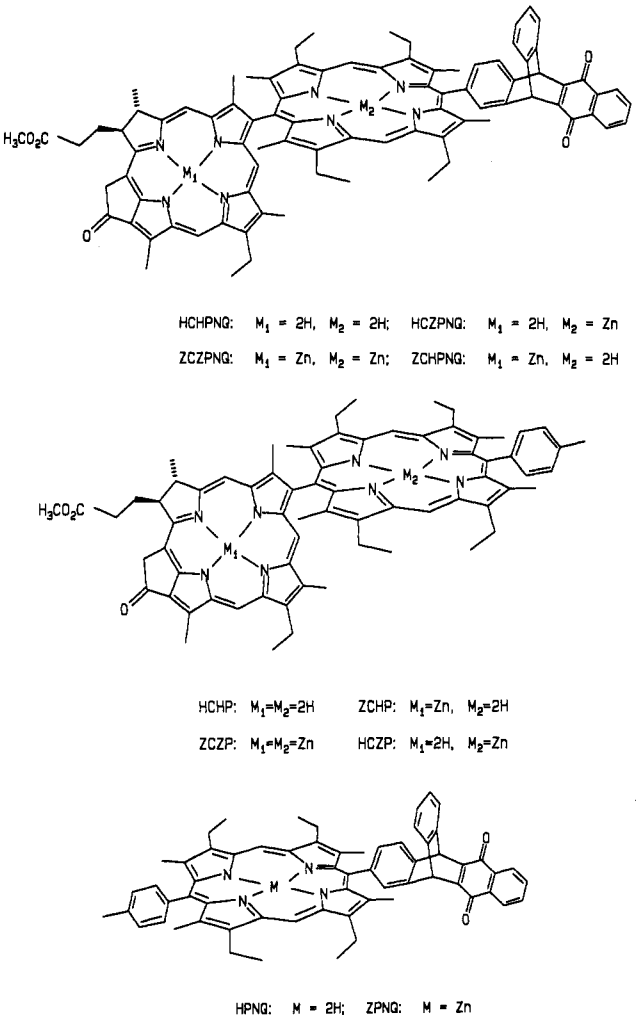

Figure 1. Structures of ZCZPNQ, ZCHPNQ, HCZPNQ, and HCHPNQ (a, top), ZCZP, ZCHP, HCZP, and HCHP (b, middle), and ZPNQ and HPNQ (c, bottom).

The central benzene ring of the spacer is either unsubstituted or possesses *p*-dimethoxy substituents. The charge separation rate constants for the molecules possessing both substituted and unsubstituted spacers are the same, while the subsequent ion-pair recombination reaction is about 3–4 times faster for the molecule with the *p*-dimethoxy-substituted spacer relative to that with the unsubstituted spacer. This difference is attributed to a superexchange interaction involving an electronic configuration of the spacer in which the dimethoxybenzene cation contributes more effectively than the benzene cation.

To better understand the influence of low-lying electronic states of the bridging molecule on electron transfer rates within chlorophyll–quinone donor–acceptor molecules, we have prepared four chlorophyll–porphyrin–quinone molecules in which the two macrocycles and the rigid quinone are positioned at a fixed distance and orientation relative to one another, Figure 1a. Center-to-center distances in these molecules are as follows: chlorophyll–

(24) Bixon, M.; Jortner, J.; Michel-Beyerle, M. E. *Biochim. Biophys. Acta* **1991**, *1056*, 301.
(25) Chan, C. K.; DiMagno, T. J.; Chen, L. X. Q.; Norris, J. R.; Fleming, G. R. *Proc. Natl. Acad. Sci. U.S.A.* **1991**, *88*, 11202.
(26) Heitele, H.; Michel-Beyerle, M. E. *J. Am. Chem. Soc.* **1985**, *107*, 8286.
(27) Heitele, H.; Michel-Beyerle, M. E. In *Antennas and Reaction Centers of Photosynthetic Bacteria*; Michel-Beyerle, M. E., Ed.; Springer: Berlin, 1985; p. 250–255.
(28) Sessler, J. L.; Johnson, M. R.; Creager, S. E.; Fettinger, J. C.; Ibers, J. A. *J. Am. Chem. Soc.* **1990**, *112*, 9310.
(29) Rodriguez, J.; Kirmaier, C.; Johnson, M. R.; Friesner, R. A.; Holten, D.; Sessler, J. L. *J. Am. Chem. Soc.* **1991**, *113*, 1652.
(30) Osuka, A.; Maruyama, K.; Mataga, N.; Asahi, T.; Yamazaki, I.; Tamai, N.; Nishimura, Y. *Chem. Phys. Lett.* **1991**, *181*, 413.
(31) Osuka, A.; Nakajima, S.; Maruyama, K.; Mataga, N.; Asahi, T. *Chem. Lett.* **1991**, 1003.
(32) Osuka, A.; Nagata, T.; Kobayashi, F.; Zhang, R. P.; Maruyama, K.; Mataga, N.; Asahi, T.; Ohno, T.; Nozaki, K. *Chem. Phys. Lett.* **1992**, *199*, 302.
(33) Wasielewski, M. R.; Niemczyk, M. P.; Johnson, D. G.; Svec, W. A.; Minsek, D. W. *Tetrahedron* **1989**, *45*, 4785.
(34) Hart, H.; Bashir-Hashemi, A.; Luo, J.; Meador, M. A. *Tetrahedron* **1986**, *42*, 1641.

porphyrin, 8.6 Å; porphyrin–quinone, 9.9 Å; chlorophyll–quinone, 18.0 Å.[35] In addition, the π system of the quinone is isolated from that of the porphyrin by a triptycene bridge. These molecules possess several important advantages in carrying out a study of this type. First, the pigment array is rigid and possesses fixed distances between the donors and acceptors. Second, the lowest excited singlet states of these molecules for the most part retain the electronic characteristics of the terminal chlorophyll molecule. Thus, the chlorophyll-like lowest excited singlet states of these molecules can be selectively excited. Thus, there is no ambiguity with regard to the initial state prior to electron transfer. Third, the π system of the quinone is electronically decoupled from that of the porphyrin to a sufficient extent to ensure non-adiabatic electron transfer and to promote relatively long-lived charge separation. Fourth, chlorophylls and porphyrins possess significantly different electronic ground, excited, and ionic state spectra. Thus, it is relatively straightforward to determine whether intermediate states involving the porphyrin bridging molecule are populated during the course of the electron transfer reactions. We have already successfully employed this approach to examine the solvent-dependent photophysics of the structurally analogous chlorophyll–porphyrin system without the quinone, Figure 1b.[36] The data from this earlier NQ-free series will serve as a reference for the new compounds discussed in this paper. We have also prepared and studied the corresponding chlorin-free porphyrin–quinone systems, Figure 1c, as reference compounds. The results presented in this paper show that there exists a wider spectrum of mechanistic possibilities for bridge-mediated electron transfer than have been observed as yet in photosynthetic reaction centers. The ability to modify the structures and energetics of model compounds in a systematic fashion makes it possible to explore additional mechanisms. An analogous approach in the reaction center protein involving site-directed mutagenesis is progressing.[37]

Results

Synthesis. The structures of HCHPNQ, HCZPNQ, ZCHPNQ, and ZCZPNQ are shown in Figure 1a. These molecules were prepared from their common free-base intermediate HCHPNQ. The porphyrinogen of HCHPNQ was prepared from methyl pyropheophorbide *d*[38] and 2-formyltriptycenenaphthoquinone[39] in a condensation reaction with 3,3′-dimethyl-4,4′-diethyldipyrrylmethane.[40] The condensation reaction was carried out using the method of Lindsey.[41] Formation of HCHPNQ from the porphyrinogen was accomplished by room temperature oxidation with chloranil.

Stirring HCHPNQ with $ZnOAc_2$ in $CHCl_3$/MeOH at room temperature metalates only the porphyrin to yield HCZPNQ, while refluxing the same solution results in metalation of both macrocycles to yield ZCZPNQ. If ZCZPNQ is treated with dichloroacetic acid, the porphyrin loses its Zn atom much more rapidly than does the chlorophyll. Thus, ZCHPNQ is readily obtained from ZCZPNQ. The proton NMR spectra of all four molecules are solvent independent. The methyl groups at the 3 and 7 positions of the porphyrin buttress the chlorophyll and fix the plane of the chlorophyll macrocycle and the plane of the triptycene benzene ring, while methyl groups at the 13 and 17 positions of the porphyrin similarly fix the 2-triptycenenaphthoquinone.[42] Thus, rotations about the single bonds joining the porphyrin to the chlorophyll and joining the porphyrin to the triptycenenaphthoquinone are completely restricted. Each molecule consists of a pair of diastereomers. These diastereomers may be separated by HPLC. However, the photophysical data presented here did not vary outside of experimental error as a function of isomer.

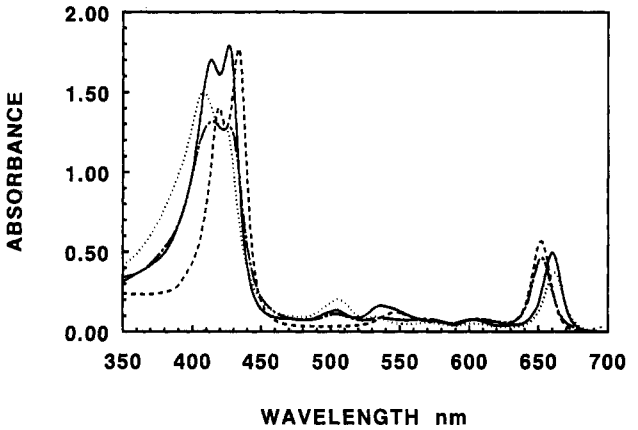

Figure 2. Ground state absorption spectra of 10^{-5} M ZCZPNQ (—), ZCHPNQ (- - -), HCZPNQ (– · –), and HCHPNQ (···) in butyronitrile.

The syntheses of the corresponding reference compounds lacking the quinone, HCHP, HCZP, ZCHP, and ZCZP (Figure 1b) are strictly analogous to those described above and have been reported previously.[36] The synthesis of HPNQ proceeds as described above, substituting *p*-tolualdehyde for the methyl pheophorbide *d*. Metalation with Zn to give ZPNQ is also analogous to that given above.

Photophysics. The ground state optical absorption spectra of all four chlorin–porphyrin–quinone triads are shown in Figure 2. The spectra of these molecules are a superposition of the respective spectra of the porphyrin and chlorophyll moieties with two Soret bands and distinct Q bands for each macrocycle. Since the energy levels of the chlorophyll and porphyrin macrocycles are nonresonant, exciton splittings of the optical absorption bands are not observed. However, a significant reduction in extinction coefficient for the porphyrin Soret band occurs, while the intensity of the chlorophyll Soret band remains comparable to that in the unlinked macrocycle.[43] The molar extinction coefficients of the porphyrin and chlorophyll Soret bands are comparable. The Q_y bands of the chlorophyll rings in ZCZPNQ and ZCHPNQ occur at 652 nm, while those of HCZPNQ and HCHPNQ occur at 661 nm and are red-shifted by 9 and 10 nm from the respective bands in zinc and free-base methyl *meso*-pyropheophorbide *a*. Similarly, the (0,0) fluorescence emission bands of both ZCZPNQ and ZCHPNQ occur at 662 nm, while those of HCZPNQ and HCHPNQ occur at 669 nm and are also red-shifted by 9 and 10 nm from the corresponding bands in zinc and free-base methyl *meso*-pyropheophorbide *a*. Thus, the π systems of the two macrocycles are weakly coupled. The lowest excited singlet states principally retain the electronic character of the chlorophyll, while the higher lying singlet states are more significantly perturbed. The large molar extinction coefficients of the chlorophyll Q bands make it possible to selectively excite this chromophore. At 610 nm, the wavelength of our laser excitation experiments, the ratio of chlorophyll/porphyrin absorbance is >25 for ZCZPNQ and HCZPNQ and about 7 for ZCHPNQ and HCHPNQ. In addition, the distinct Soret bands of the chlorophyll and porphyrin can be used to monitor the involvement of chlorophyll and/or

(35) The distances were determined from MM2 energy minimized structures using HyperChem software.

(36) Wasielewski, M. R.; Johnson, D. G.; Niemczyk, M. P.; Gaines, G. L., III; O'Neil, M. P.; Svec, W. A. *J. Am. Chem. Soc.* **1990**, *112*, 6482.

(37) Chan, C. K.; Chen, L. X. Q.; DiMagno, T. J.; Hanson, D. K.; Nance, S. L.; Schiffer, M.; Norris, J. R.; Fleming, G. R. *Chem. Phys. Lett.* **1991**, *176*, 366.

(38) Johnson, D. G.; Svec, W. A.; Wasielewski, M. R. *Isr. J. Chem.* **1988**, *28*, 193.

(39) Wasielewski, M. R.; Niemczyk, M. P. *J. Am. Chem. Soc.* **1984**, *106*, 5043.

(40) Bullock, E.; Johnson, A. W.; Markham, E.; Shaw, K. B. *J. Chem. Soc.* **1958**, 1430.

(41) Lindsey, J. S.; Wagner, R. W. *J. Org. Chem.* **1989**, *54*, 828.

(42) Wasielewski, M. R.; Niemczyk, M. P.; Svec, W. A.; Pewitt, E. B. *J. Am. Chem. Soc.* **1985**, *107*, 5583.

(43) We have recently measured Raman excitation profiles for the bichromophoric XCXP molecule. These results unequivocally assign the longer wavelength Soret band to the chlorophyll and the shorter wavelength Soret band to the porphyrin.

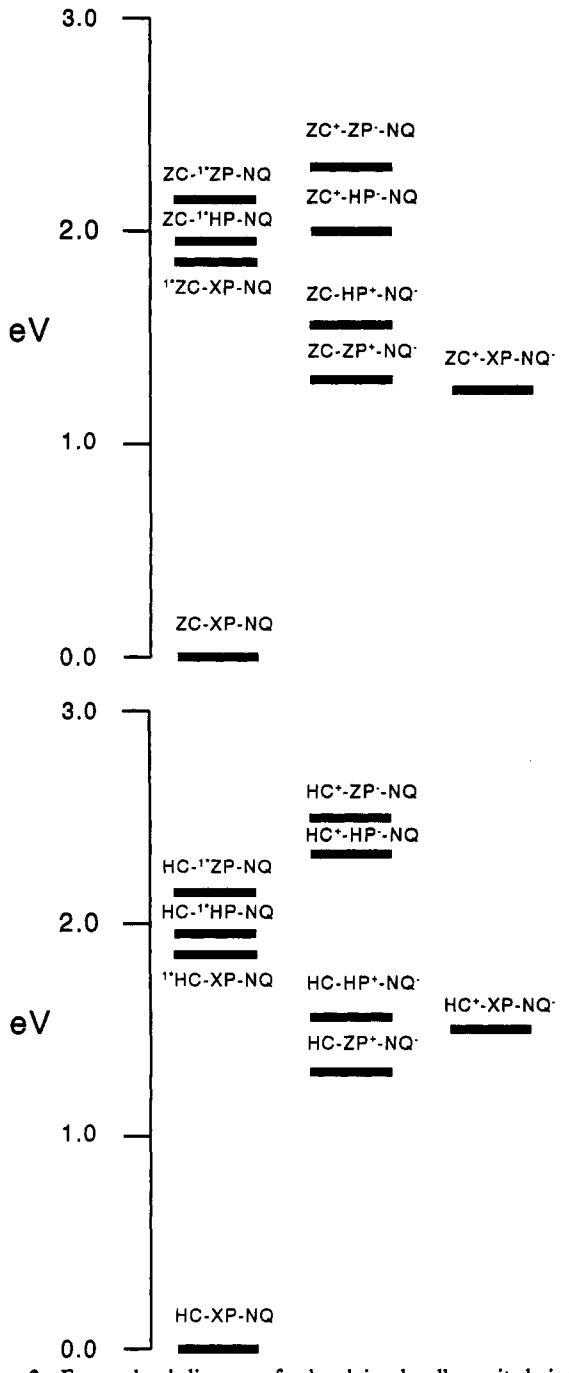

Figure 3. Energy level diagrams for low-lying locally excited singlet states and charge transfer states of ZCHPNQ and ZCZPNQ in butyronitrile (a, top) and HCHPNQ and HCZPNQ in butyronitrile (b, bottom).

porphyrin states following selective excitation of the chlorophyll in these molecules.

Figure 3a shows the energy levels of the locally excited states of the chromophores within ZCZPNQ and ZCHPNQ along with several of their hypothetical ion-pair states. Figure 3b shows the same information for HCZPNQ and HCHPNQ. The energies of the excited states are determined from the positions of the corresponding (0,0) fluorescence bands of these molecules in butyronitrile, while the ion-pair state energies are estimated from the sum of the one-electron oxidation and reduction potentials of the donors and acceptors in butyronitrile. The ion-pair state energies in butyronitrile are reasonably good estimates of the true ion-pair state energies because the ions are strongly solvated, and the Coulombic interaction between ions separated by ≈10 Å is small in highly polar media. Figure 3 shows that ion-pair states with anionic character on the porphyrin are low-lying virtual states, while ion-pair states with cationic character on the porphyrin lie below the locally excited singlet states of the macrocycles.

The fluorescence quantum yields and lifetimes of ZCZPNQ, ZCHPNQ, HCHPNQ, HCZPNQ, HCNQ, ZPNQ, ZC, and HC in butyronitrile are given in Table I. The fluorescence quantum yields and lifetimes of the chlorophyll–porphyrin–quinone molecules are all significantly diminished relative to those for ZC and HC. In addition, the fluorescence quantum yields of ZCZPNQ, ZCHPNQ, and HCHPNQ are all significantly less than those of the corresponding quinone-free molecules. Moreover, the fluorescence quantum yields of these molecules decrease proportionally as their observed fluorescence lifetimes decrease. This suggests that a non-radiative channel dependent on the presence of the porphyrin and/or quinone competes with radiative decay. The nature of this channel can be examined by looking for transient spectral changes that arise following excitation of the quinone-containing molecules.

Figure 4 compares the transient absorption difference spectrum of ZCZPNQ with that of ZCHPNQ from 380 to 480 nm and from 620 to 840 nm. The spectra are obtained 20 ps following excitation by a 1 ps, 610 nm laser flash. In each compound the Soret band due to the chlorophyll chromophore at 430 nm bleaches within the 1 ps time of the laser flash. There is only a weak bleach at 415 nm at times >1 ps. This may be due to excited state mixing between the chlorophyll and the porphyrin, or it may represent loss in intensity of the vibronic bands due to the chlorophyll alone. Similarly, the chlorophyll Q_y bands bleach immediately upon excitation. In addition, weak positive absorption changes occur throughout the near-infrared. Both the lowest excited singlet state and the radical ion states of chlorophyll are known to absorb at these wavelengths.[44-46]

Figure 5 reports similar data for HCZPNQ and HCHPNQ. The spectra are obtained 5 ps following excitation of HCZPNQ and 100 ps following excitation of HCHPNQ. Once again, the Soret bands due to the chlorophyll macrocycles bleach within the time of the laser flash. There is evidence of weak bleaching near 415 nm in HCHPNQ. However, the 415-nm band in HCZPNQ bleaches strongly within 5 ps of the laser flash. This observation is similar to that made for HCZP that lacks NQ.[36] In both HCZPNQ and HCHPNQ the chlorophyll Q_y bands bleach immediately upon excitation. Figure 5 shows that HCZPNQ has a significant positive ΔA contribution from 620–800 nm, while HCHPNQ shows substantially weaker absorption in this region. These spectra are also similar to those already reported for HCZP and for HCHP containing no appended NQ.[36]

If S_1 of a molecule is significantly populated in a picosecond transient absorption experiment, the weak probe light may stimulate the excited molecules to emit. This behavior often results in the appearance of a negative ΔA feature in the transient absorption spectrum at wavelengths at which there is little or no ground state absorption.[45] This stimulated emission feature can be used to measure the lifetime of S_1. Figure 6 shows the decay of the stimulated emission from ZCZPNQ, ZCHPNQ, HCZPNQ, and HCHPNQ as a function of time. The data for ZCZPNQ and ZCHPNQ are monitored at 665 nm. The fits to the data yield single exponential decay times of 10 ± 1 and 110 ± 5 ps. The emission band for HCZPNQ recovers with a single exponential time of 8 ± 2 ps at 677 nm. The rising absorption feature that appears beyond 20 ps is due to the appearance of HC^-ZP^+NQ, which is not completely selected against at 677 nm. The transient absorption due to HC^-ZP^+NQ will be discussed in detail below. The recovery of the stimulated emission from

(44) Borg, D. C.; Fajer, J.; Felton, R. H.; Dolphin, D. *Proc. Natl. Acad. Sci. U.S.A.* **1970**, *67*, 813.
(45) Rodriguez, J.; Kirmaier, C.; Holten, D. *J. Am. Chem. Soc.* **1989**, *111*, 6500.
(46) Fujita, I.; Davis, M. S.; Fajer, J. *J. Am. Chem. Soc.* **1978**, *100*, 6280.

Table I. Photophysical Data

compd	ϕ_F	τ_F(ns)	k_{et}(s^{-1})	k_{cr}(s^{-1})
HC	0.17 ± 0.01	9.4 ± 0.4		
ZC	0.22 ± 0.01	6.00 ± 0.01		
HPNQ	0.0012 ± 0.0001	0.0080 ± 0.0008	$1.1 \pm 0.2 \times 10^{11}$	$5.6 \pm 0.2 \times 10^{9}$
ZPNQ	0.0009 ± 0.0001	<0.006	$9.6 \pm 0.6 \times 10^{11}$	$3.2 \pm 0.3 \times 10^{11}$
HCHPNQ	0.014 ± 0.001	0.122 ± 0.004	$8.2 \pm 0.1 \times 10^{9}$	$4.0 \pm 0.1 \times 10^{9}$
HCZPNQ	0.0007 ± 0.0004	0.0070 ± 0.0006	$1.2 \pm 0.1 \times 10^{11}$	$2.5 \pm 0.1 \times 10^{10}$
ZCHPNQ	0.019 ± 0.001	0.109 ● 0.004	$9.0 \pm 0.1 \times 10^{9}$	$4.0 \pm 0.1 \times 10^{9}$
ZCZPNQ	0.0025 ± 0.0004	0.012 ± 0.003	$1.0 \pm 0.2 \times 10^{11}$	$1.4 \pm 0.1 \times 10^{10}$

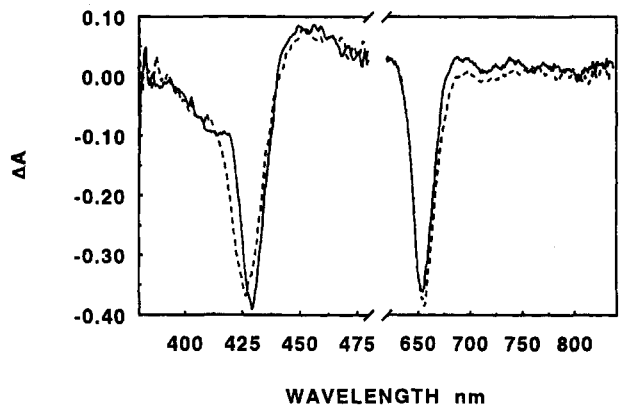

Figure 4. Transient absorption spectra in the regions 380–480 and 620–840 nm of ZCZPNQ (—) and ZCHPNQ (- - -) in butyronitrile at 20 ps following a 1 ps laser flash at 610 nm.

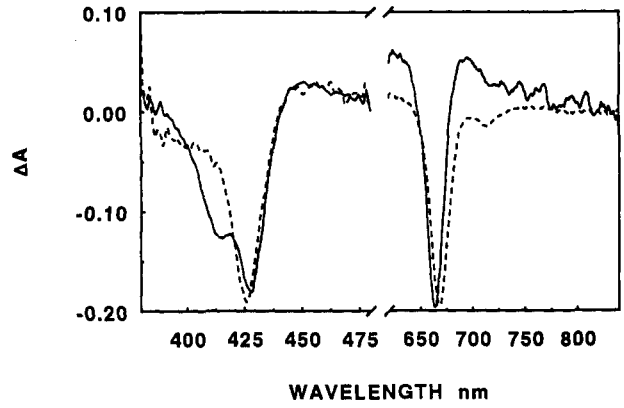

Figure 5. Transient absorption spectra in the regions 380–480 and 620–840 nm of HCZPNQ (—) at 5 ps and HCHPNQ (- - -) at 100 ps in butyronitrile following a 1 ps laser flash at 610 nm.

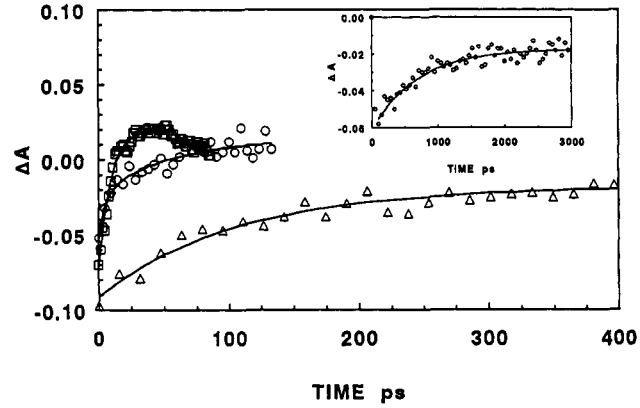

Figure 6. Transient recovery of stimulated emission at 665 nm for ZCZPNQ (○) and ZCHPNQ (△) and at 677 for HCZPNQ (□). Inset: Same at 715 nm for HCHPNQ (○). All data were obtained in butyronitrile following a 1 ps, 610 nm laser flash.

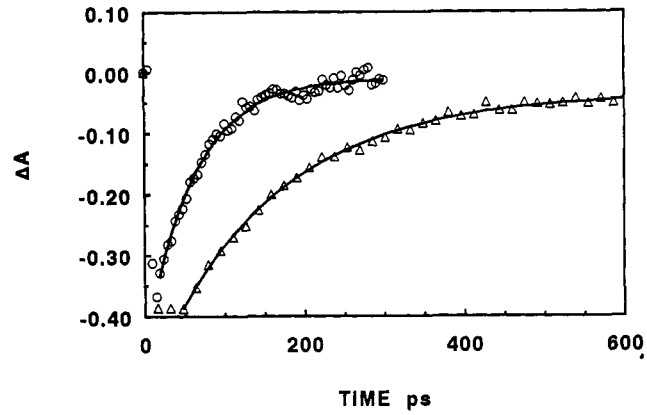

Figure 7. Transient absorption decay of ZCZPNQ (○) and ZCHPNQ (△) in butyronitrile at 652 nm following a 1 ps laser flash at 610 nm.

HCHPNQ is monitored at the (1,0) vibronic band at 715 nm. This emission feature is readily seen in the spectrum displayed in Figure 5. Monitoring stimulated emission via the (1,0) vibronic band eliminates the convolution of the stimulated emission feature with the bleach of the absorption band inherent in monitoring the (0,0) transition in chlorophylls. The single exponential recovery time is 690 ± 50 ps. These data are in excellent agreement with the S_1 lifetimes determined directly by fluorescence decay measurements and reported in Table I.

We can determine the forward electron transfer rate from these data using eq 1:

$$k_{et} = (1/\tau_X) - (1/\tau_{ZC \text{ or } HC}) \quad (1)$$

where k_{et} is the charge separation rate constant for compound X, $\tau_{ZC \text{ or } HC}$ is the fluorescence lifetime of ZC or HC, and τ_X is the fluorescence or stimulated emission lifetime of X. With use of eq 1 the charge separation rate constants for ZCZPNQ, ZCHPNQ, HCHPNQ, and HCZPNQ are given in Table I.

Figure 7 shows the time dependence for the recovery of the Q_y band bleach at 652 nm for ZCZPNQ and ZCHPNQ. Note that the respective recovery times are substantially longer than the S_1 lifetimes for each molecule. Thus, the ground state recovery kinetics monitored by the disappearance of transient absorption changes in the Q_y bands must reflect not only S_1 decay but both the formation and decay of a state that is much longer lived than S_1. Similar kinetics for absorption recovery are obtained for the 430-nm Soret bands. The absorption features in the 750–840-nm portion of the spectrum decay with kinetics similar to those of the Q_y bands. However, the small magnitude of the absorption changes between 750 nm and 840 nm preclude their use to accurately determine rate constants. Nevertheless, the fact that these changes persist longer than the lifetimes of S_1 support the idea that the weak absorption changes in the near-infrared are due to a state produced from S_1, most likely ZC^+ZPNQ^- and ZC^+HPNQ^-.

A corresponding data set for HCZPNQ and HCHPNQ is presented in Figure 8. This figure shows the recovery of the 661-nm transient absorption for HCHPNQ. Once again the recovery of the Q_y band bleach is slower than the decay time of S_1, Table I. Figure 9 shows both the formation and decay kinetics

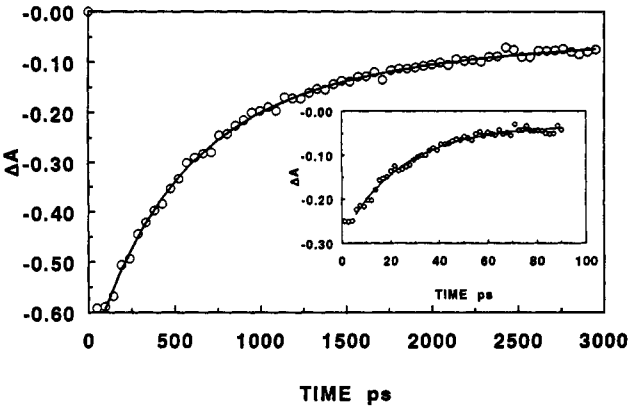

Figure 8. Transient absorption decay of HCHPNQ. Inset: Same of HCZPNQ. All data were obtained in butyronitrile at 661 nm following a 1 ps laser flash at 610 nm.

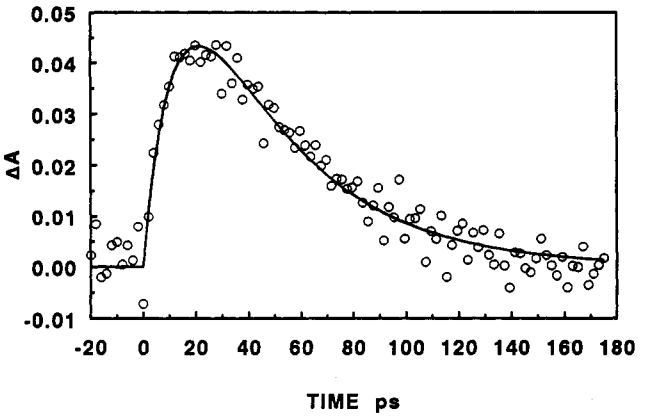

Figure 9. Transient absorption changes for HCZPNQ in butyronitrile at 688 nm following a 1 ps laser flash at 610 nm.

for HC^-ZP^+NQ at 688 nm. At this wavelength ZP^+ possesses significant absorption, whereas the S_1 state of HCZPNQ does not.[47]

Included in Table I are important data for reference compounds ZPNQ and HPNQ. Note that in both of these molecules the rate constants for charge recombination are significantly faster than those observed for the corresponding XCZPNQ and XCHPNQ derivatives, where X is either H or Z.

The charge separation and recombination rate constants presented in Table I assume a series mechanism:[33] ^{1}*XCXPNQ $\rightarrow$ XC^+XPNQ^- $\rightarrow$ XCXPNQ. The charge separation rate constants are obtained from the decay of S_1 using eq 1, and the charge recombination rate constants are obtained from the fit of the recovery of the absorption spectra illustrated in Figures 4 and 5 using the series mechanism. Throughout their recovery time the spectral features illustrated in Figures 4 and 5 only diminish. No new features or changes in band shape or structure are observed. In addition, the transient spectra and their rapid recovery both suggest that chlorophyll and porphyrin triplet states do not play a role in the photochemistry of the NQ-containing molecules in butyronitrile.

Discussion

The results presented above suggest that the presence of the quinone induces a new non-radiative path for the deactivation of S_1 in these molecules. The kinetic and spectroscopic data show that a new state with a longer lifetime than that of S_1 is formed. We assign this state to the charge separated product that results from rapid electron transfer from the lowest excited singlet states of ZCZPNQ, ZCHPNQ, and HCHPNQ to yield the oxidized chlorophyll and reduced quinone. The presence or absence of a Zn atom in the central porphyrin has a large influence on the observed rate constants for both charge separation and recombination. The discussion that follows examines the possible mechanisms for chlorophyll–quinone electron transfer mediated by the central bridging porphyrin.

The transient absorption changes in the Soret region of the spectrum for XCXPNQ molecules are particularly informative with regard to the creation of excited and/or ionic states involving either the chlorophyll or the porphyrin. Our transient absorption spectra for ZCZPNQ and ZCHPNQ, Figure 4, show that the chlorophyll Soret bands near 430 nm bleach following excitation. The observed transient absorption spectra show only weak bleaching at the porphyrin Soret band near 415 nm throughout the time course of the ensuing photochemistry. The degree of bleaching at 415 nm relative to that at 430 nm does not change significantly within the time resolution of the experiment. The same statement can be made for HCHPNQ shown in Figure 5. Whenever porphyrins or chlorophylls leave their respective ground states, the Soret band bleaches to some extent. While this bleach is non-specific with regard to assigning excited state or ionic state characteristics to the porphyrin or chlorophyll, our recently published work on the quinone-free XCXP derivatives shows that charge separation within these bichromophoric pairs results in a bleach of both Soret bands, while formation of the lowest excited singlet state of this pair results principally in bleaching of the chlorophyll Soret band.[36] This is consistent with the fact that S_1 for the chlorophyll is lower in energy than that of the porphyrin. Examination of the transient absorption spectrum of HCZPNQ in Figure 5 shows that the porphyrin Soret band near 415 nm is strongly bleached. This is consistent with the formation of HC^-ZP^+NQ as dictated by the favorable energetics of this process and noted in the Results section above.

In the remaining XCXPNQ molecules we can identify and discuss four potential electronic mechanisms for photochemical electron transfer from the lowest excited singlet state of the chlorophyll to the quinone. In addition, we recognize that structural differences may exist between HP and ZP that result in changes in the electronic coupling matrix elements in electron transfer mechanisms that utilize orbitals localized on the porphyrin. The electronic spectrum of the porphyrin in each XCXPNQ molecule remains only slightly perturbed from that of the porphyrin itself. It is well-known that serious distortions of the porphyrin structure result in significant changes to the porphyrin spectra.[48] However, we cannot easily assess the influence of small changes at this time. Since the electronic properties of the bridging porphyrin in the XCXPNQ molecules change dramatically upon substitution of the central Zn atom, we will focus the remaining discussion on the possible influence of these changes on the observed electron transfer reactions within these molecules.

First, the electron transfer reaction may occur in two steps using the porphyrin bridging molecule as a reduced intermediate. However, this mechanism can be completely ruled out by energetic considerations. Figure 3 shows that all states in which the porphyrin is reduced lie above the lowest excited singlet states of the chlorophyll donors. Thus, the free energy of reaction for the initial photochemical reduction of the central bridging porphyrin is always positive. The only molecule of this series in which the chlorophyll–porphyrin macrocyclic pair itself undergoes electron transfer to form ion-pair intermediates in butyronitrile is HCZPNQ. We observed an 8 ps 1/e time for the formation of the ion-pair state, HC^-ZP^+NQ, which lives for 40 ps, Figure 9. This is consistent with our earlier observations of HC^-ZP^+ after excitation of HCZP.[36] The free energy of formation of HC^-ZP^+ from ^{1}*HCZPNQ within HCZPNQ is –0.1 eV. Thus,

(47) Fajer, J.; Borg, D. C.; Forman, A.; Dolphin, D.; Felton, R. H. *J. Am. Chem. Soc.* **1970**, *92*, 3451.

(48) Barkigia, K.; Berber, M. D.; Fajer, J.; Medforth, C. J.; Renner, M. W.; Smith, K. M. *J. Am. Chem. Soc.* **1990**, *112*, 8851.

the direction of electron transfer in HCZPNQ is opposite to that of the other three compounds in Figure 1a and need not be considered further in a discussion of the effectiveness of the porphyrin bridge in promoting electron transfer from ZC or HC to NQ.

The second possibility is that electron transfer within ZCZPNQ, ZCHPNQ, and HCHPNQ occurs via a superexchange mechanism using virtual states that place the electron on the porphyrin. In this case the rates of electron transfer should depend on the energies of the ZC^+HP^-NQ, ZC^+ZP^-NQ, and HC^+HP^-NQ virtual charge transfer states indicated in Figure 3, parts a and b. Using a second-order perturbation theory treatment of superexchange,[2] the coupling of virtual states ZC^+ZP^-NQ and ZC^+HP^-NQ to ^{1}*ZC and HC^+HP^-NQ to ^{1}*HC depends on $1/\Delta E^2$, where ΔE is the vertical energy gap between ^{1}*ZC or ^{1}*HC and the corresponding ionic virtual states evaluated at the crossing point between the potential surfaces for the initial ^{1}*ZC or ^{1}*HC excited state and the corresponding ZC^+XPNQ^- or HC^+HPNQ^- product state. Examination of Figure 3a shows that ZC^+HP^-NQ is about 0.15 eV above ^{1}*ZC, while ZC^+ZP^-NQ is about 0.4 eV above ^{1}*ZC. Similarly, Figure 3b shows that HC^+HP^-NQ is about 0.4 eV above ^{1}*HC. Assuming simple parabolic potentials these energetics suggest that a superexchange mechanism for charge separation involving reduced states of the bridging porphyrin should lead to a charge separation rate constant for ZCHPNQ that is approximately 7 times faster than that of ZCZPNQ and HCHPNQ. However, this predicted ordering of rate constants is exactly opposite to the order we observe. Our data show that ZCZPNQ undergoes charge separation *about 11 times faster* than does ZCHPNQ. In addition, the rate constant for charge separation in HCHPNQ is very similar to that of ZCHPNQ.

The third and fourth mechanistic possibilities involve mixing between the locally excited states of the chlorophyll and the porphyrin within XCXPNQ. The ground state absorption spectra of the XCXPNQ molecules, Figure 2, show that the chlorin Q_y absorption bands of molecules containing ZC occur at 652 nm. These bands are red shifted by 9 nm relative to the corresponding Q_y band of zinc methyl *meso*-pyrochlorophyllide *a*, which possesses an ethyl group at the 3 position. Similarly, the chlorin Q_y bands of the molecules containing HC occur at 661 nm, once again red-shifted by 10 nm from that of methyl *meso*-pyropheophorbide *a*. In addition, the Soret bands of the porphyrins in the XCXPNQ molecules are diminished in intensity relative to those of the chlorophylls. Normally, the molar extinction coefficients for porphyrin Soret bands are about 4 times larger than those for chlorophylls. These spectral changes suggest that weak mixing occurs between the lowest excited singlet states of the chlorophylls and the porphyrins within the XCXPNQ series. The resultant mixed chlorophyll–porphyrin lowest excited state possesses an electronic structure that strongly resembles that of the chlorophyll, while placing excited state character on the porphyrin.

Thus, the third possible mechanism for the role of the bridging porphyrin that we wish to discuss focuses on the possibility that a mixed chlorophyll–porphyrin lowest excited singlet state may participate in a superexchange interaction with states in which the porphyrin is reduced. Examination of parts a and b of Figure 3 shows that the states in which the porphyrin is reduced lie above the locally excited states of the corresponding XCXPNQ molecules. Thus, this variant of the superexchange mechanism predicts that the molecules possessing the free-base porphyrin should undergo charge separation faster than their zinc porphyrin counterparts. This is once again contrary to our observations.

In the preceding discussion we have neglected states of these molecules that place positive charge on the porphyrin. The fourth possible mechanism for the influence of the porphyrin bridging molecule on the rate of electron transfer that we wish to consider is the role of the states $ZCZP^+NQ^-$, $ZCHP^+NQ^-$, and $HCHP^+NQ^-$ in this process. Assuming that weak mixing between the chlorophyll and porphyrin lowest excited singlet states occurs, one may consider a mechanism for electron transfer wherein the mixed excited state decays to an intermediary charge transfer state, which then decays rapidly to yield the product state ZC^+ZPNQ^-; for example, ^{1}*(ZCZP)NQ → $ZCZP^+NQ^-$ → ZC^+ZPNQ^-. This mechanism was originally proposed as a possible explanation for the role of the intermediary bacteriochlorophyll in photosynthetic reaction centers.[49] The ground state optical absorption spectra of the XCXPNQ molecules suggest that the degree of excited state mixing between either ^{1}*HC or ^{1}*ZC and either of the porphyrin excited states ^{1}*HP or ^{1}*ZP is to a first approximation similar. On the other hand, the Franck–Condon factors for the reaction ^{1}*(ZCZP)NQ → $ZCZP^+NQ^-$ should be greater than those for the reaction ^{1}*(ZCHP)NQ → $ZCHP^+NQ^-$. This is a consequence of energy gap considerations. The energy levels of the various ionic intermediates given in parts a and b of Figure 3 assume that the ionic states are fully relaxed and solvated by the surrounding medium. While this is certainly true for the final products that live for 70-250 ps, there is some question as to the energy of intermediates that live for <5 ps. This point will be discussed more fully below. Nevertheless, given fully relaxed intermediates, the energy of $ZCZP^+NQ^-$ is 0.85 eV below that of ^{1}*ZP, which is close to the typical 1 eV total reorganization energy for electron transfer reactions involving these species and spacers,[50] while the energy of $ZCHP^+NQ^-$ is only 0.42 eV below that of ^{1}*HP. Thus, any admixture of porphyrin excited state character into ^{1}*ZC should improve Franck–Condon overlap for reactions involving the metalloporphyrin bridge more so than for those in which the bridge is a free-base porphyrin. The larger energy gap for ZCZPNQ relative to that for both ZCHPNQ and HCHPNQ suggests that the charge separation reaction should be much faster for ZCZPNQ than for ZCHPNQ and HCHPNQ. Moreover, this mechanism also predicts that the charge separation rate constants for ZCHPNQ and HCHPNQ should be comparable. This is exactly what we observe.

The intermediate charge transfer states with positive charge on the porphyrin bridging molecule may be real or virtual intermediates. Our data indicate that for times >1 ps no significant buildup of intermediates involving the porphyrin occurs. Therefore, if real intermediates containing oxidized porphyrins are produced in these reactions, their lifetimes are most likely <1 ps. This fact suggests that the electronic coupling between the oxidized porphyrin and the neutral chlorin is very large, and consequently, the electron transfer reaction $XCXP^+NQ^-$ → XC^+XPNQ^- may be adiabatic. If this reaction is adiabatic, its rate may be controlled by solvent dynamics. Moreover, under this circumstance the energies of the intermediate states possessing charged porphyrins depicted in parts a and b of Figure 3 may no longer be valid. Several criteria for determining the adiabaticity of electron transfer reactions can be applied to the reaction $XCXP^+NQ^-$ → XC^+XPNQ^-. The expression for the non-adiabatic electron transfer rate constant at high temperatures is given by eq 2.[51]

$$k = (2\pi V^2/\hbar)(4\pi\lambda k_B T)^{-1/2} \exp[-\Delta G/k_B T] \qquad (2)$$

where V is the electronic coupling matrix element, λ is the total reorganization energy, ΔG is the free energy, T is the temperature, k_B is Boltzmann's constant, and $\hbar$ is Planck's constant. Since the free energy for the oxidation of the chlorin by the porphyrin cation is only –0.15 eV, eq 2 predicts that V must be at least 4000 cm^{-1} to obtain a rate constant $>10^{12}$ s^{-1}. This result is nonsensical because eq 2 was developed for non-adiabatic reactions in which V is assumed to be substantially smaller.

(49) Fischer, S. F.; Scherer, P. O. *J. Chem. Phys.* **1987**, *115*, 151.
(50) Wasielewski, M. R.; Niemczyk, M. P.; Svec, W. A.; Pewitt, E. B. *J. Am. Chem. Soc.* **1985**, *107*, 1080.
(51) Marcus, R. A. *J. Chem. Phys.* **1965**, *43*, 679.

Electron transfer reactions are non-adiabatic by Landau–Zener criteria if they satisfy the relationship[52-54]

$$2\pi V^2/\hbar\omega(2\lambda k_B T)^{1/2} < 1 \qquad (3)$$

where ω is the characteristic frequency of the medium and the other parameters are defined above. For typical low-frequency solvent motions, $\omega \sim 100\ cm^{-1}$ at 300 K, and a total reorganization energy of about 1 eV, which is typical of the types of molecules discussed here, eq 3 predicts that V must be $<145\ cm^{-1}$. Since the rate of electron transfer from the chlorin to the porphyrin cation is $>10^{12}\ s^{-1}$, it is quite likely that the coupling between these two molecules is sufficiently large to make the reaction adiabatic. Thus, if the low-lying ionic states of the chlorin and porphyrin are strongly coupled, it is possible that mixing of these states results in an overall charge transfer state in which strong polarization of charge toward the chlorin occurs. This makes it difficult to obtain a distinct spectroscopic signature for the porphyrin in the overall electron transfer process.

If the electron transfer reaction $XCXP^+NQ^- \rightarrow XC^+XPNQ^-$ is adiabatic with $V > 100\ cm^{-1}$, then one may apply the adiabaticity criterion of Rips and Jortner[55] to determine whether solvent dynamics will have a large influence on the reaction rate. The adiabaticity parameter, K, is given by

$$K = 4\pi V^2 \tau_L/\hbar\lambda \qquad (4)$$

where τ_L is the longitudinal relaxation time of the solvent and the other parameters are defined above. For a non-adiabatic reaction $K \ll 1$, and the reaction rate is independent of solvent dynamics. Thus, applying eq 4 to the reaction $XCXP^+NQ^- \rightarrow XC^+XPNQ^-$, if $V > 100\ cm^{-1}$ in butyronitrile for which $\tau_L = 1.7$ ps, $K > 5$. Thus, the rate constant for the reaction $XCXP^+NQ^- \rightarrow XC^+XPNQ^-$ is probably solvent controlled. In keeping with the fact that a hypothetical $XCXP^+NQ^-$ intermediate must live for <1 ps, it is likely that this species is not fully solvated, and thus, the energetics in parts a and b of Figure 3 are incorrect. We can estimate the energy level of the $XCXP^+NQ^-$ intermediates by recognizing that the solvent contribution to the nuclear reorganization energy of the electron transfer reaction is $\lambda_s \sim 0$, when the rate of electron transfer is $>1/\tau_L$. Using the Born dielectric continuum model of the solvent, Weller has shown that the free energy of an ion-pair is destabilized by about 0.6 eV for the radii of and distances between XC and XP, when $\lambda_s \sim 0$.[56] Thus, Figure 3, parts a and b, can be modified to give Figure 10, parts a and b. In Figure 10a note that the energy level of $ZCHP^+NQ^-$ is above the energies of the lowest excited singlet states of both ZC and HP, whereas $ZCZP^+NQ^-$ is isoenergetic with ^{1}*ZC and below the energy of ^{1}*ZP. This suggests again that the reaction ^{1}*(ZCXP)NQ $\rightarrow$ $ZCXP^+NQ^-$ should be more rapid for X = Zn than for X = H. A similar argument can be made for HCHPNQ.

The charge recombination rates in the XCXPNQ series can be analyzed in a straightforward fashion using a superexchange mechanism. Figure 10 shows that the energies of the intermediate states $ZCZP^+NQ^-$, $ZCHP^+NQ^-$, and $HCHP^+NQ^-$ are sufficiently far above those of ZC^+XPNQ^- and HC^+XPNQ^- to preclude thermal population of these states in a two-step charge recombination reaction. On the other hand, a superexchange mechanism utilizing the states $ZCZP^+NQ^-$, $ZCHP^+NQ^-$, and $HCHP^+NQ^-$ can adequately account for the fact that the molecule with the ZP-bridging molecule returns to ground state 3.5 times faster than do both molecules that possess HP bridges. These rate constants are consistent with the fact that the energy gap between $ZCZP^+NQ^-$ and ZC^+ZPNQ^- is smaller than that between $ZCHP^+NQ^-$ and ZC^+HPNQ^-. Similar considerations hold for $HCHP^+NQ^-$ and HC^+HPNQ^-.

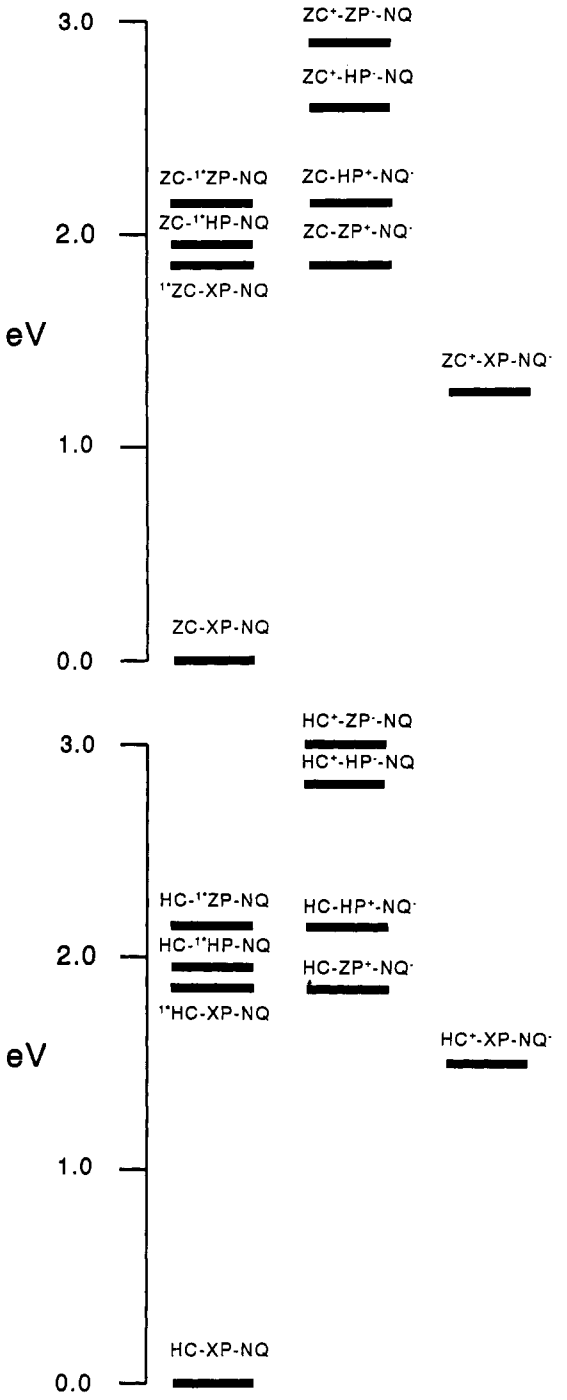

Figure 10. Energy level diagrams for low-lying locally excited singlet states and charge transfer states of ZCHPNQ and ZCZPNQ in butyronitrile (a) and HCHPNQ and HCZPNQ in butyronitrile (b) assuming weak solvation of the charge transfer states with charges on the porphyrins.

Conclusion

The chlorophyll–porphyrin–naphthoquinone molecules described in this paper undergo rapid photoinduced electron transfer. During the course of both charge separation and recombination, at no time >1 ps do we see evidence for significant buildup of an intermediate ionic state on the porphyrin. Nevertheless, both the charge separation and recombination reactions for ZCZPNQ are significantly faster than those for ZCHPNQ and HCHPNQ. This observation is inconsistent with models of superexchange in

(52) Kubo, R.; Toyozawa, Y. *Prog. Theor. Phys.* **1955**, *13*, 160.
(53) Levich, V. G.; Dogonadze, R. R. *Dokl. Acad. Nauk SSSR* **1959**, *124*, 123.
(54) Levich, V. G. *Adv. Electrochem. Eng.* **1965**, *4*, 249.
(55) Rips, I.; Jortner, J. *J. Chem. Phys.* **1987**, *87*, 2090.
(56) Weller, A. *Z. Phys. Chem. N.F.* **1982**, *133*, 93.

which low-lying virtual states of the type ZC^+ZP^-NQ and ZC^+HP^-NQ influence the rates of electron transfer that produce either ZC^+ZPNQ^- or ZC^+HPNQ^-. However, the data are consistent with a model in which mixing between the chlorophyll and porphyrin lowest excited states enhances the influence of states such as $ZCZP^+NQ^-$, $ZCHP^+NQ^-$, and $HCHP^+NQ^-$ in determining the overall rate of electron transfer. It may prove useful to examine current models of superexchange in biological electron transfer reactions in light of these data.

Experimental Section

Physical Measurements. Solvents for all spectroscopic experiments were dried and stored over 3 Å molecular sieves. Butyronitrile was refluxed over $KMnO_4$ and Na_2CO_3 and then twice distilled, retaining the middle portion each time.

Proton NMR spectra were obtained on a 300-MHz Bruker spectrometer. UV–visible absorption spectra were taken on a Shimadzu UV-160. Fluorescence spectra were obtained using a Perkin-Elmer MPF-2A fluorimeter interfaced to an IBM PC computer. All samples for fluorescence were purified by preparative TLC on Merck silica gel plates. Samples for fluorescence measurements were 10^{-7} M in 1-cm cuvettes. The emission was measured 90° to the excitation beam. Fluorescence quantum yields were determined by integrating the digitized emission spectra from 600 to 800 nm and referencing the integral to that for chlorophyll *a* in diethyl ether.[57]

Redox potentials for ZCZPNQ and ZCHPNQ were determined in butyronitrile containing 0.1 M tetra-*n*-butylammonium perchlorate using a Pt disk electrode at 21°. These potentials were measured relative to a saturated calomel electrode using ac voltammetry.[58] Both the one electron oxidations and reductions of these molecules exhibited good reversibility.

The transient absorption spectra were obtained using a Rh-6G dye laser synchronously pumped by a frequency-doubled, mode-locked cw Nd-YAG laser. The 1.0-ps pulses of 610-nm light were amplified by a 4-stage dye amplifier (Rh-640) pumped by the frequency doubled output (532 nm) of a Nd:YAG laser possessing a 10 Hz repetition rate. Malachite green saturable absorber dye jets between stages 2 and 3 and between stages 3 and 4 of the amplifier chain minimized the amplified stimulated emission generated in the amplifier. The amplification produced 1 mJ/pulse at 10 Hz. This beam was sent through a 60/40 beam splitter. The smaller portion was focused down to a 2 mm diameter beam and used as the excitation pulse. The larger portion was tightly focused into a 2 cm path length cell containing either 2/1 $CCl_4/CHCl_3$ or 1/1 H_2O/D_2O. This generated a continuum which was used as the probe light. The arrival at the sample of the probe beam was delayed relative to the excitation beam by an optical delay. The probe beam was divided into reference and measuring beams by a 50/50 beam splitter. Both probe beams passed through the sample. The reference beam passed through an area that was not illuminated by the excitation beam, while the measuring beam passed through the same portion of the sample through which the excitation beam passed. Both beams were then focused onto the slit of a ISA HR-320 monochromator. The monochromator dispersed the beams onto the face of an intensified SIT detector which was part of an optical multichannel analyzer (PAR OMA II). Solutions with an absorbance of about 0.15 at 610 nm (2 mm pathlength cells) were used.

Fluorescence lifetime measurements used 1.0 ps, 2 mm diameter, 200 μJ pulses from the same source as described for the transient absorbance experiments. The samples were placed in 0.5-cm cells (optical density ca. 0.03 at 610 nm) and emission 90° to the excitation was collected and focused onto the slit of a Hamamatsu C979 streak camera. The temporally dispersed image was recorded by the intensified SIT vidicon of the PAR OMA II. The geometry of the experimental setup determined the 15 ps instrument response. Decay times were obtained by iterative reconvolution of the data with least-squares fitting using the Levenberg–Marquardt algorithm.

Syntheses. (a) HCHPNQ. A 2.5-mL portion of a stock solution of 4,4′-diethyl-3,3′-dimethyldipyrrylmethane[37] (1.44 g in 10 mL of chloroform; 0.36 g, 1.5×10^{-3} mol), 2-formyltriptycenenaphthoquinone[36] (0.54 g, 1.5×10^{-3} mol), and methyl pyropheophorbide *d*[35] (0.4 g, 7.25×10^{-4} mol) are added to 150 mL of chloroform under nitrogen with stirring at room temperature. The solution is purged with nitrogen for ~2 min. Boron trifluoride etherate (0.2 mL) is added, and the mixture is stirred for 2 h. The reaction is conveniently followed by TLC in 10% acetone in chloroform (v/v). A greenish-brown band ($R_f \sim 0.7$) forms quickly. This is the porphyrinogen precursor to the product. Chloranil (0.35 g, 1.5×10^{-3} mol) is added and the mixture is stirred for 0.5 h. The organic layer is then stripped on a rotary evaporator and column chromatographed with 5% acetone in methylene chloride (v/v). All fractions containing the product are rechromatographed with 2% acetone in methylene chloride (v/v): 0.12 g isolated, 14% yield. Electronic spectrum (butyronitrile): λ_{max} (rel ϵ) 408 (1.000), 422 (0.923), 506 (0.138), 532 (0.065), 570 (0.045), 603 (0.048), 661 nm (0.296). NMR ($CDCl_3$): (triptycenenaphthoquinone group) δ 8.18–8.30 (m, 3 H), 7.82–7.95 (m, 2 H), 7.81 (m, 2 H), 7.73 (d, 1 H, J = 7.8 Hz), 7.62 (d, 1 H, J = 7.8 Hz), 7.22 (m, 2 H), 6.39 (s, 1 H), 6.25 (s, 1 H); (porphyrin) δ 10.34 (s, 2 H), 4.07 (q, 4 H, J = ~7.4 Hz), ~3.92 (m, 4 H), 2.57 (s, 6 H), 1.91 (s, 3 H), 1.87 (s, 3 H), 1.82 (t, 6 H, J = 7.6 Hz), 1.68 (t, 6 H, J = 7.13 Hz); (phorbin) δ 9.50 (s, 1 H), 8.89 (s, 1 H), 8.84 (s, 1 H), 5.40 and 5.24 (AB quartet, 2 H, J = 20.1 Hz), 4.47 (d, 1 H, J = 8.6 Hz), 4.69 (q, 1 H, J = 7.1 Hz), 4.47 (d, 1 H, J = 8.6 Hz), 3.72 (s, 3 H), 3.69 (s, 3 H), 3.47 (q, 2 H, J = 7.5 Hz), 3.18 (s, 3 H), ~2.80 (m, 3 H), ~2.48 (m, 2 H), 2.23 (s, 3 H), 2.03 (d, 3 H, 7.2 Hz); ring NH's –1.00 (br s, 4 H). Mass spectrum (FAB) calcd 1330 (M), found 1334 (M + 4).

(b) HCZPNQ. HCHPNQ (50 mg, 3.8×10^{-5} mol) is dissolved in a mixture of 3/1 v/v chloroform/methanol (25 mL) with stirring under nitrogen. Zinc acetate dihydrate (15 mg, 6.9×10^{-5} mol) is added and a rapid color change from green-brown to red-brown occurs. The porphyrin ring now contains zinc. The reaction mixture is poured into water and extracted with chloroform, and the organic layer is washed twice with water, dried over anhydrous potassium carbonate, and stripped on a rotary evaporator. Preparatory TLC on C_{18}-reverse phase plates and elution with 20% chloroform in methanol separates the HCZPNQ from minor amounts of HCHPNQ, ZCHPNQ, and ZCZPNQ. Yield: 94%. Electronic spectrum (butyronitrile): λ_{max} (rel ϵ) 414 (1.000), 427 (0.928), 505 (0.062), 537 (0.097), 604 (0.026), 660 nm (0.280). NMR ($CDCl_3$): (triptycenenaphthoquinone group) δ 8.18–8.30 (m, 3 H), 7.82–7.95 (m, 2 H), 7.81 (m, 2 H), 7.73 (d, 1 H, J = 7.8 Hz), 7.62 (d, 1 H, J = 7.8 Hz), 7.22 (m, 2 H), 6.39 (s, 1 H), 6.25 (s, 1 H); (porphyrin) δ 10.29 (s, 2 H), 4.07 (q, 4 H, J = ~7.4 Hz), ~3.87 (m, 4 H), 2.56 (s, 6 H), 1.90 (s, 3 H), 1.86 (s, 3 H), 1.81 (t, 6 H, J = 7.6 Hz), 1.67 (t, 6 H, J = 7.13 Hz); (phorbin) δ 9.51 (s, 1 H), 8.892 (s, 1 H), 8.72 (s, 1 H), 5.40 and 5.23 (AB quartet, 2 H, J = 20.1 Hz), 4.47 (d, 1 H, J = 8.6 Hz), 4.69 (q, 1 H, J = 7.1 Hz), 4.47 (d, 1 H, J = 8.6 Hz), 3.71 (s, 3 H), 3.68 (s, 3 H), 3.46 (q, 2 H, J = 7.5 Hz), 3.17 (s, 3 H), ~2.80 (m, 3 H), ~2.48 (m, 2 H), 2.23 (s, 3 H), 2.02 (d, 3 H, 7.2 Hz); ring NH's ~–1.00 (br s, 2 H).

ZCZPNQ. HCHPNQ (50 mg, 3.8×10^{-5} mol) is dissolved in a mixture of 3/1 v/v chloroform/methanol (25 mL) with stirring under nitrogen. Zinc acetate dihydrate (20 mg, 9.2×10^{-5} mol) is added and the solution is refluxed for 1 h. A deep green color signifies that both the chlorophyll and porphyrin rings are metalated. The workup is identical to that of HCZPNQ above. Yield 98%. Electronic spectrum (butyronitrile): λ_{max} (rel ϵ) 419 (1.000), 433 (1.087), 547 (0.087), 606 (0.064), 652 nm (0.332). NMR ($CDCl_3$): (triptycenenaphthoquinone group): δ 8.18–8.30 (m, 3 H), 7.82–7.95 (m, 2 H), 7.81 (m, 2 H), 7.73 (d, 1 H, J = 7.8 Hz), 7.62 (d, 1 H, J = 7.8 Hz), 7.22 (m, 2 H), 6.39 (s, 1 H), 6.25 (s, 1 H); (porphyrin) δ 10.29 (s, 2 H), 4.07 (q, 4 H, J = ~7.4 Hz), ~3.87 (m, 4 H), 2.57 (s, 6 H), 1.90 (s, 3 H), 1.86 (s, 3 H), 1.81 (t, 6 H, J = 7.6 Hz), 1.67 (t, 6 H, J = 7.13 Hz); (phorbin) δ 9.58 (s, 1 H), 8.73 (s, 1 H), 8.71 (s, 1 H), 5.40 and 5.24 (AB quartet, 2 H, J = 20.1 Hz), 4.47 (d, 1 H, J = 8.6 Hz), 4.69 (q, 1 H, J = 7.1 Hz), 4.47 (d, 1 H, J = 8.6 Hz), 3.71 (s, 3 H), 3.68 (s, 3 H), 3.46 (q, 2 H, J = 7.5 Hz), 3.17 (s, 3 H), ~2.80 (m, 3 H), ~2.48 (m, 2 H), 2.23 (s, 3 H), 2.03 (d, 3 H, 7.2 Hz).

ZCHPNQ. ZCZPNQ (10 mg, 6.8×10^{-6} mol) is dissolved in methylene chloride (10 mL). Dichloroacetic acid (10 μL) is added with stirring. A light green color occurs immediately signifying release of the zinc from the porphyrin ring. The solution is stirred for 1 h and then poured into dilute, aqueous potassium carbonate. The organic layer is washed twice with water, dried over anhydrous potassium carbonate, and stripped on a rotary evaporator. Preparatory TLC on C_{18}-reverse phase plates and elution with 20% chloroform in methanol results in a clean separation of ZCHPNQ from residual HCHPNQ, HCZPNQ, and ZCZPNQ. Yield 6.5 mg, 68%. Electronic spectrum (butyronitrile): λ_{max} (rel ϵ) 414 (1.000), 426 (1.112), 505 (0.101), 536 (0.070), 570 (0.064), 606 (0.067), 652 nm (0.509). NMR ($CDCl_3$): (triptycenenaphthoquinone group) δ 8.18–8.30 (m, 3 H), 7.82–7.95 (m, 2 H), 7.81 (m, 2 H), 7.73 (d, 1 H, J = 7.8 Hz), 7.62 (d, 1 H, J = 7.8 Hz), 7.22 (m, 2 H), 6.39 (s, 1 H), 6.25 (s,

(57) Latimer, P.; Bannister, T. T.; Rabinowitch, E. *Nature* **1956**, *124*, 585.
(58) Wasielewski, M. R.; Smith, R. L.; Kostka, A. G. *J. Am. Chem. Soc.* **1980**, *102*, 6923.

1 H); (porphyrin) δ 10.34 (s, 2 H), 4.07 (q, 4 H, J = ~7.4 Hz), ~3.92 (m, 4 H), 2.57 (s, 6 H), 1.90 (s, 3 H), 1.86 (s, 3 H), 1.81 (t, 6 H, J = 7.6 Hz), 1.67 (t, 6 H, J = 7.13 Hz); (phorbin) δ 9.58 (s, 1 H), 8.73 (s, 1 H), 8.71 (s, 1 H), 5.40 and 5.24 (AB quartet, 2 H, J = 20.1 Hz), 4.47 (d, 1 H, J = 8.6 Hz), 4.69 (q, 1 H, J = 7.1 Hz), 4.47 (d, 1 H, J = 8.6 Hz), 3.71 (s, 3 H), 3.68 (s, 3 H), 3.46 (q, 2 H, J = 7.5 Hz), 3.17 (s, 3 H), ~2.80 (m, 3 H), ~2.48 (m, 2 H), 2.23 (s, 3 H), 2.03 (d, 3 H, J = 7.2 Hz); ring NH's −1.00 (br s, 2 H).

HPNQ. A 2.5-mL portion of a stock solution of 4,4′-diethyl-3,3′-dimethyldipyrrylmethane[37] (1.44 g in 10 mL of chloroform; (0.36 g, 1.5 × 10^{-3} mol), 2-formyltriptycenenaphthoquinone[36] (0.27 g, 7.5 × 10^{-4} mol), and p-tolualdehyde (0.09 g, 7.5 × 10^{-4} mol) are added to 150 mL of CH_2Cl_2 under nitrogen with stirring at room temperature. The solution is purged with nitrogen for ~2 min. Trifluoroacetic acid (0.55 g) is added, and the mixture is stirred for 2 h. Chloranil (0.35 g, 1.5 × 10^{-3} mol) is added and the mixture is stirred for 0.5 h. The organic layer is then stripped on a rotary evaporator and column chromatographed with 5% acetone in methylene chloride (v/v). All fractions containing the product are rechromatographed with 2% acetone in methylene chloride (v/v): 0.16 g isolated, 22% yield. Electronic spectrum (butyronitrile): λ_{max} (rel ε) 408 (1.000), 505 (0.138), 540 (0.065), 590 (0.045), 620 nm (0.048). NMR ($CDCl_3$): (triptycenenaphthoquinone group) δ 8.18–8.30 (m, 3 H), 7.82–7.95 (m, 2 H), 7.81 (m, 2 H), 7.73 (d, 1 H, J = 7.8 Hz), 7.62 (d, 1 H, J = 7.8 Hz), 7.22 (m, 2 H), 6.39 (s, 1 H), 6.25 (s, 1 H); (porphyrin) δ 10.34 (s, 2 H), 4.07 (q, 4 H, J = ~7.4 Hz), ~3.92 (m, 4 H), 2.57 (s, 6 H), 1.91 (s, 3 H), 1.87 (s, 3 H), 1.82 (t, 6 H, J = 7.6 Hz), 1.68 (t, 6 H, J = 7.13 Hz); (p-tolyl) δ 8.01 (d, 1 H, J = 7.9 Hz), 7.95 (d, 1 H, J = 7.8 Hz), 7.58 (d, 2 H, J = 7.8 Hz), 2.75 (s, 3 H), ~2.50 (s, 2 H, NH); mass spectrum (FAB) calcd 900 (M), found 904 (M + 4).

ZPNQ. HPNQ (50 mg, 3.8 × 10^{-5} mol) is dissolved in a mixture of 3/1 v/v chloroform/methanol (25 mL) with stirring under nitrogen. Zinc acetate dihydrate (15 mg, 6.9 × 10^{-5} mol) is added and a rapid color change from red-brown to bright red occurs. The porphyrin ring now contains zinc. The reaction mixture is poured into water and extracted with chloroform, and the organic layer is washed twice with water, dried over anhydrous potassium carbonate, and stripped on a rotary evaporator. Yield: 98%. Electronic spectrum (butyronitrile): λ_{max} (rel ε) 418 (1.000), 548 (0.055), 580 nm (0.009). NMR ($CDCl_3$): (triptycenenaphthoquinone group) δ 8.18–8.30 (m, 3 H), 7.82–7.95 (m, 2 H), 7.81 (m, 2 H), 7.73 (d, 1 H, J = 7.8 Hz), 7.62 (d, 1 H, J = 7.8 Hz), 7.22 (m, 2 H), 6.39 (s, 1 H), 6.25 (s, 1 H); (porphyrin) δ 10.29 (s, 2 H), 4.07 (q, 4 H, J = ~7.4 Hz), ~3.87 (m, 4 H), 2.56 (s, 6 H), 1.90 (s, 3 H), 1.86 (s, 3 H), 1.81 (t, 6 H, J = 7.6 Hz), 1.67 (t, 6 H, J = 7.13 Hz); (p-tolyl) δ 8.01 (d, 1 H, J = 7.9 Hz), 7.95 (d, 1 H, J = 7.8 Hz), 7.58 (d, 2 H, J = 7.8 Hz), 2.75 (s, 3 H).

Acknowledgment. The authors acknowledge the support of the Division of Chemical Sciences, Office of Basic Energy Sciences, U.S. Department of Energy under contract W-31-109-Eng-38.